



Structural investigation on nano-crystalline Cu–Cr supersaturated solid solution prepared by mechanical alloying

S. Sheibani*, S. Heshmati-Manesh, A. Ataie

School of Metallurgy and Materials Engineering, University of Tehran, Tehran, Iran

ARTICLE INFO

Article history:

Received 17 December 2009
Received in revised form 28 January 2010
Accepted 5 February 2010
Available online 16 February 2010

Keywords:

Mechanical alloying
Solid solution
Nano-crystalline
X-ray diffraction

ABSTRACT

In this paper, elemental Cu–7 wt.% Cr powder mixture was mechanically alloyed in order to study the solid solubility extension during the alloying process. By mechanical alloying in a high energy ball mill, a nano-structured and homogeneous Cu–Cr powder was obtained. The effect of toluene as a process control agent (PCA) was investigated. The structural changes were characterised by X-ray diffraction (XRD) technique. The Gibbs free energy change in this system during the formation of solid solution was calculated and shown to be positive, which means that a thermodynamic barrier exist for the formation of this alloy system in solid state. It was found that the additional energy stored in the nano-crystalline Cu–Cr alloy during mechanical alloying process as a result of crystallite size reduction and increased dislocation density, would be high enough to overcome the thermodynamic barrier in the formation of a solid solution.

© 2010 Elsevier B.V. All rights reserved.

1. Introduction

Cu–Cr alloys have wide application potential in the automobile, electrical and electronic industries due to their high electrical conductivity and high mechanical strength. Solid solution formation and further precipitation of Cr in Cu matrix have already been used to produce in situ copper matrix composite. Extensive studies are now being carried out on this in situ composite which have much higher concentrations of the secondary element than the dilute Cu alloys [1–4]. Hence, attainment of supersaturated Cr in Cu matrix, which has limited solubility at equilibrium state, is of interest.

Extension of solubility range would be possible by non-equilibrium processing methods. Among different methods, mechanical alloying has been attracted a lot of attention in recent years. Mechanical alloying is a simple method that transfers high amount of energy to the powder during the milling process. Also, during the mechanical alloying, intense deformation is introduced into the particles. This is manifested by the presence of a variety of crystal defects such as dislocations, vacancies, stacking faults, and increased number of grain boundaries. Furthermore, by mechanical alloying it is possible to obtain nano-crystalline materials [5,6].

It has already been shown that the limit of solid solubility in Cu–Cr system can be increased by mechanical alloying [7–10]. Further development requires better understanding of the process through characterization of the products. But detailed study of solid solubility extension has not been thoroughly investigated. Also, the influence of PCA on this process has not been studied yet.

In this work, the solid solubility extension of Cr in Cu by mechanical alloying has been studied with special focus on the thermodynamic aspects of the whole process and Gibbs free energy changes. Unlike the previous work reported by Aguilar et al. [11] who studied Cu–Cr supersaturated solid solution formation using modified Warren–Averbach method, results presented in this paper are based on Williamson–Hall method in XRD profile analysis.

2. Experimental procedure

Starting materials were commercially pure Cu (99%, <75 μm), Cr (99.5%, <75 μm) and toluene (Merck, extra pure) as the process control agent. The samples with a nominal composition of Cu–7 wt.% Cr were prepared in a planetary ball mill, using hardened steel vials and balls, under argon atmosphere, to prevent oxidation. The ball to powder weight ratio and milling speed were 30:1 and 300 rpm, respectively. In order to study the effect of PCA on the solid solution formation, the milling process of some samples was carried out with 1 wt.% toluene.

The structural evolution in the powder during milling was investigated by XRD using a Philips PW-3710 diffractometer with Co K α radiation. The crystallite size and internal strains of powder were determined according to the Williamson–Hall plot [12]. The line broadening due to the instrument was calculated from Warren's method [13,14]. The lattice parameters were calculated from XRD data. High angle reflections (1 1 1), (2 0 0), (3 3 1) and (2 1 0) were used to determine the lattice parameters. The true lattice parameter of the specimen was determined by a least square regression of the values calculated from each reflection against $\cos \theta \cot \theta$, taking lattice parameter as the intercept of the regression line [2].

* Corresponding author at: School of Metallurgy and Materials Engineering, University of Tehran, P.O. Box 14395-1491, Tehran, Iran. Tel.: +98 912 1958219; fax: +98 21 88006076.

E-mail address: ssheibani@ut.ac.ir (S. Sheibani).

3. Thermodynamic analysis

A thermodynamic analysis was carried out to predict the more stable phase and to compare with mechanical alloying results. Considering the formation of the disordered A(B) solid solution from a mixture of pure A and B elements (as the standard state), the Gibbs free energy change can be presented as [15]:

$$\Delta G^S = \Delta H_m^S - T\Delta S^S \quad (1)$$

where, ΔH_m^S and ΔS^S are the enthalpy and entropy of mixing, respectively. T is the temperature at which a solid solution is formed. Also, for the formation of solid solution from elemental powders, ΔS^S can be calculated with the assumption of configurational entropy of mixing:

$$\Delta S^S = -R(x_A \ln x_A + x_B \ln x_B) \quad (2)$$

where, R is the universal gas constant, and x_A and x_B are the mole fractions of elements A and B, respectively.

According to Miedema's semi-empirical model, the enthalpy of formation of a solid solution consists of three terms [16]:

$$\Delta H_m^S = \Delta H_{\text{chemical}} + \Delta H_{\text{elastic}} + \Delta H_{\text{structural}} \quad (3)$$

where, $\Delta H_{\text{chemical}}$ is the chemical contribution, which is the same for liquid and solid solutions. $\Delta H_{\text{elastic}}$ represents the elastic mismatch energy due to size mismatch, and $\Delta H_{\text{structural}}$ represents the lattice stability energy due to the difference in valence electrons and crystal structure of solute and solvent atoms. $\Delta H_{\text{chemical}}$ for binary A–B alloy can be calculated as [16]:

$$\Delta H_{\text{chemical}} = \frac{2Pf(C^S)(x_A V_A^{2/3} + x_B V_B^{2/3})}{(n_{ws}^A)^{-1/3} + (n_{ws}^B)^{-1/3}} \times \left[-(\Delta\Phi^*)^2 + \frac{Q}{P}(\Delta n_{ws}^{1/3})^2 - \frac{S}{P} \right] \quad (4)$$

where, Φ^* , V and n_{ws} are the work function, the molar volumes and the electron density of constituent elements, respectively. P , Q and S are empirical constants related to constituents and $f(C^S)$ is the concentration function that for solid solutions is given by Eqs. (5) and (6).

$$f(C^S) = C_A^S C_B^S \quad (5)$$

$$C_A^S = \frac{x_A V_A^{2/3}}{x_A V_A^{2/3} + x_B V_B^{2/3}}, \quad C_B^S = \frac{x_B V_B^{2/3}}{x_A V_A^{2/3} + x_B V_B^{2/3}} \quad (6)$$

The elastic contribution of enthalpy can be expressed as [17]:

$$\Delta H_{\text{elastic}} = x_A x_B (x_A \Delta E_{A \text{ in } B} + x_B \Delta E_{B \text{ in } A}) \quad (7)$$

where, $\Delta E_{A \text{ in } B}$ and $\Delta E_{B \text{ in } A}$ are the elastic energy caused by A dissolving in B and B dissolving in A, respectively. They can be calculated by

$$\Delta E_{A \text{ in } B} = \frac{2K_A \cdot G_B (\Delta V)^2}{3K_A \cdot V_B + 4G_B V_A} \quad \text{and} \quad \Delta E_{B \text{ in } A} = \frac{2K_B \cdot G_A (\Delta V)^2}{3K_B \cdot V_A + 4G_A V_B} \quad (8)$$

where, K and G are the bulk and shear modulus, respectively.

$\Delta H_{\text{structural}}$ is related to the number of valence electrons per atom. This is a small positive value and can be neglected in the estimation.

Since during mechanical alloying the formation of an amorphous alloy is possible, the mixing enthalpy in this state, $\Delta H_{\text{amorphous}}$, can be determined by Eq. (9). For an amorphous alloy both the elastic and structural enthalpies can be neglected, because there is no crystal structure and the atoms can arrange themselves in such a way that mismatch is avoided [16–18].

$$\Delta H_{\text{amorphous}} = \Delta H_{\text{chemical}} + \alpha T_{\text{fuse}} \quad (9)$$

Table 1

Required parameters for thermodynamic analysis according to Miedema's model in Cu–Cr system [16–18].

	Cu	Cr
$n_{ws}^{1/3}$ (cm ⁻¹)	1.47	1.73
Φ^* (V)	4.45	4.65
K (10 ¹⁰ N m ⁻²)	13.7	16.02
G (10 ¹⁰ N m ⁻²)	4.8	11.53
V (cm ³ mol ⁻¹)	7.1	7.12
T_m (K)	1357.6	2130

$$P = 14.1 \text{ kJ V}^{-2} \text{ cm}^{-1}, S/P = 0 \text{ and } Q/P = 9.4.$$

where, $\alpha = 3.5 \text{ J mol}^{-1} \text{ K}^{-1}$ and T_{fuse} is defined as:

$$T_{\text{fuse}} = x_A T_m^A + x_B T_m^B \quad (10)$$

where, T_m is the melting temperatures of A and B elements.

Therefore, the enthalpy, entropy and Gibbs free energy changes for formation of a disordered solid solution and an amorphous alloy in terms of x_A and x_B can be calculated. The required parameters in Eqs. (1)–(10) for the Cu–Cr alloy system are given in Table 1. The calculated results at 298 K are shown in Fig. 1.

Fig. 1 shows that the elastic contribution is small. This is due to the small difference in Cr and Cu atomic sizes. This can be found from molar volume values in Table 1. However, chemical enthalpy is the dominant contribution of enthalpy for solid solution formation due to the difference between bonding energy at initial state and solid solution in Cu–Cr system. Gibbs free energy change for crystalline solid solution and amorphous phase formation is positive at all compositions and there is no driving force to form these phases from the elemental components. Consequently, formation of them needs an external energy. Furthermore, the Gibbs free energy change of amorphous formation is higher than that of the crystalline solid solution; i.e. the solid solution is more stable than amorphous phase. This result is relatively in agreement with the calculation by the CALPHAD method in the literature [19].

4. Results and discussion

4.1. Effect of PCA

Fig. 2 shows the XRD patterns of the mechanically alloyed powder mixtures milled either with PCA or without it. It can be seen

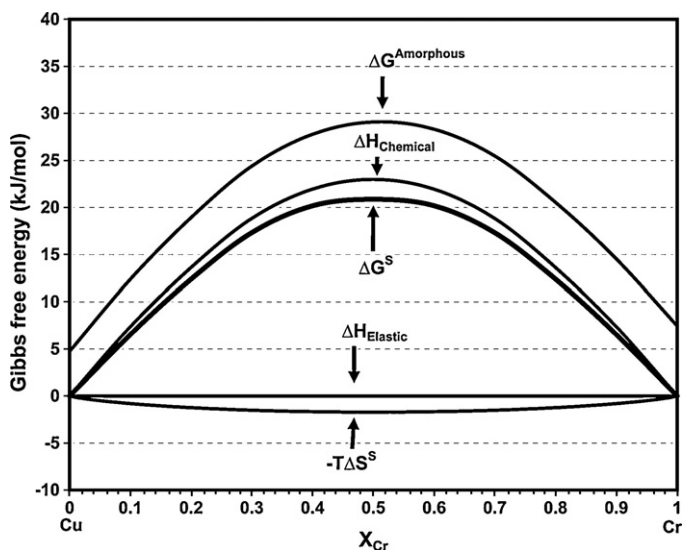


Fig. 1. Enthalpies, entropy and Gibbs free energy change for the formation of solid solution and amorphous phase in Cu–Cr system.

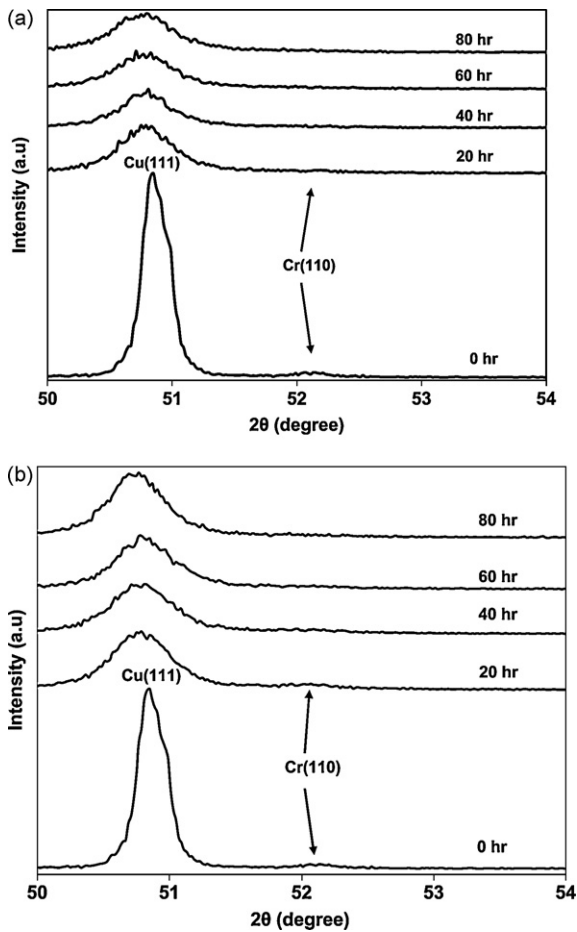


Fig. 2. XRD patterns of the powder mixture after different milling times (a) without PCA and (b) with PCA.

in both figures that, the diffraction peak of Cr is visible in the early stages of milling. However, the Cr diffraction peak diminished with increased milling time. Also, a shift of the Cu peak to lower θ angle was observed, which is related to the increase of the lattice parameter. This shift is more pronounced when milling is carried out in presence of PCA in Fig. 2(b). Also, Fig. 2(b) shows that after milling for 20 h, the diffraction peak for Cr can hardly be detected and it disappeared completely after 40 h of milling. Meanwhile, the Cu peaks broadened with increased milling time.

For more detailed study on the effect of PCA on the peaks displacement, the Cu lattice parameter changes as a function of milling time for samples milled with and without PCA are shown in Fig. 3. Comparing these figures, it can be found that there are two differences between two samples. Firstly, the lattice parameter changes more regularly for the sample processed in the presence of PCA. Secondly, in samples milled for 80 h with and without PCA, the lattice parameter increases from 0.36157 to 0.36355 and 0.36317 nm, respectively. This shows that the milling process in presence of PCA is more effective. These phenomena can be possibly explained by the preventing effect of PCA on excessive cold welding of Cu particles during the milling. Therefore, Cr dissolution in Cu matrix becomes more homogeneous.

Furthermore, the final lattice parameter of the sample milled for 80 h with PCA is in good agreement with the previous relationship between the lattice parameter and alloy composition established for supersaturated solid solution samples produced by rapid solidification [2]. Full solid solubility of Cr in Cu had been confirmed by detailed microstructural study in these samples. Therefore, our results show that a Cu–7 wt.% solid solution was formed during

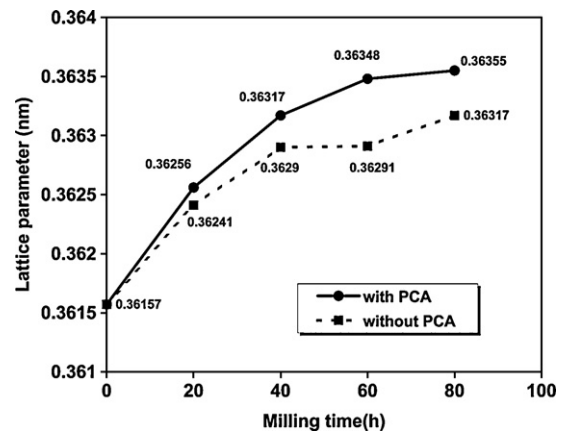


Fig. 3. Comparison of Cu lattice parameter changes as a function of milling time with PCA and without it.

milling in presence of PCA. It should be noted that, the only evidence of solid solubility extension was lattice parameter changes.

4.2. Estimation of Gibbs free energy changes

It is clear that dislocations increase the elastic energy of metals [20]. The total strain energy due to the presence of dislocations in materials, ΔG_S , can be estimated from Eq. (11) [21].

$$\Delta G_S = \zeta \rho V_E \quad (11)$$

where, ρ and V_m are the dislocation density and the molar volume, respectively. ζ is the dislocation elastic energy per unit length of dislocation line which is estimated from the following equation [20]:

$$\zeta = \left(\frac{Gb^2}{4\pi} \right) \ln \left(\frac{R_e}{b} \right) \quad (12)$$

where, G is the shear modulus, b is the burger's vector and R_e is the outer cut-off radius, taken as crystallite size in nano-crystalline materials [22]. Furthermore, ρ in the mechanically alloyed powders may be calculated from the crystallite size, D , and microstrain, ϵ , measured by XRD using Eq. (13) [23,24].

$$\rho = \frac{2\sqrt{3}\langle \epsilon^2 \rangle^{1/2}}{(D \times b)} \quad (13)$$

On the other hand, the Gibbs free energy increase due to the crystallite size decrease, ΔG_b , can be estimated from Eq. (14) [21].

$$\Delta G_b = \gamma \left(\frac{A}{V} \right) V_m \quad (14)$$

where, $\gamma = 625 \text{ mJ m}^{-2}$ is the grain boundary energy for copper and A/V is the surface/volume ratio. The crystalline morphology was considered spherical.

Fig. 4 shows the Gibbs free energy changes due to the crystallite size decrease and dislocation density increase during the milling in presence of PCA. In Fig. 4(a) typical decrease of crystallite size of metals during mechanical alloying was shown, in which the crystallite size decreased to 9 nm after 80 h of milling. This decrease leads to an approximate increase of 2.96 kJ/mol in Gibbs free energy. Fig. 4(b) shows the increase of dislocation density and Gibbs free energy up to $3 \times 10^{17} \text{ m}^{-3}$ and 2.08 kJ/mol, respectively. If the maximum values of the Gibbs free energy changes from crystallite size and dislocation density were taken into account, the total Gibbs free energy would be 5.04 kJ/mol. A comparison between this value and the Gibbs free energy of mixing curve in Fig. 1 shows that, 80 h of mechanical alloying process has provided the required energy to

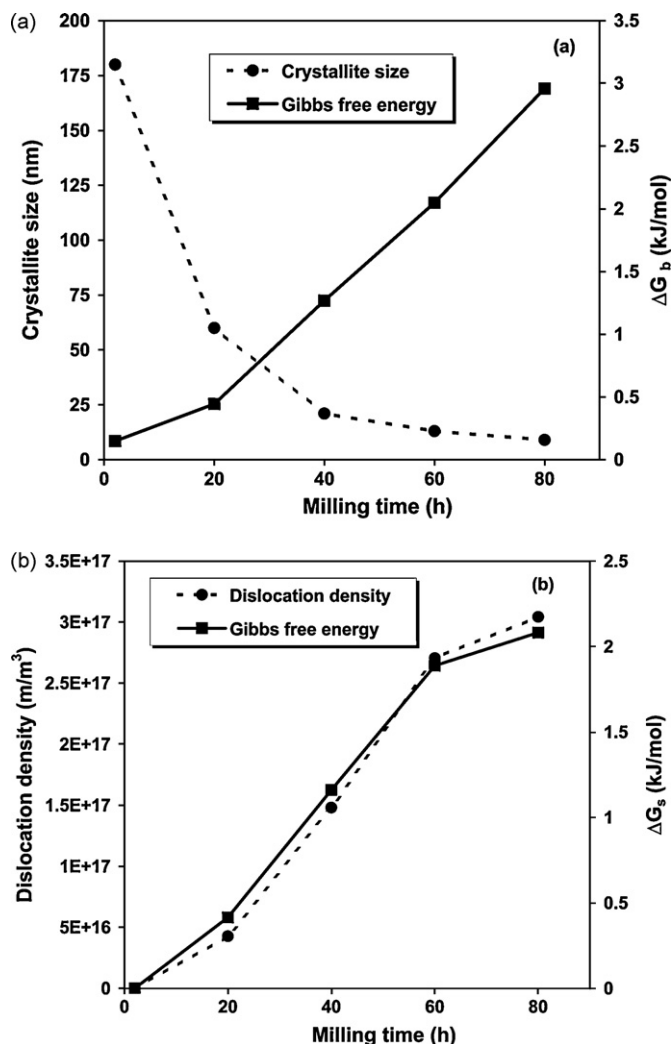


Fig. 4. (a) Crystallite size and ΔG_b , and (b) microstrain and ΔG_s versus milling time with PCA.

extend the solid solubility of Cr in Cu. Therefore, a reduction of the crystallite size and increase of the dislocation density will increase the free energy and consequently raise the equilibrium Cr solubility limit in the Cu crystal lattice.

The estimated total Gibbs free energy is smaller than the value obtained from Fig. 1 for the composition of 7 wt.% Cr, i.e. 6 kJ/mol. The difference between estimated values of Gibbs free energy from XRD data and thermodynamic analysis may be explained by the following reasons:

Errors in the crystallite size and microstrain measurements from XRD data.

Increase of internal temperature of powder mixture up to a level higher than the presumed 298 K. Because the thermodynamic barrier energy will be lower for calculation at higher temperature. Introduction of other types of defects in the crystal lattice during the milling process which may result in more free energy increase. However, in the present results only dislocations were taken into account.

The structural evolution and related calculation of another constituent, i.e. Cr, was neglected because of the limitations in the XRD peaks analysis.

Based on the results presented in Fig. 4, the free energy contribution due to the decrease of crystallite size is higher than dislocation density, as reported by others [11]. But, in the estimation, only one mean crystallite size was considered which is inaccurate since the crystallite size in many nano-crystalline materials presents a log-normal distribution [11]. So the fraction of crystallite with small sizes was not contributed.

In comparison with an earlier report on Cu–Cr system, based on XRD profile analysis by Warren–Averbach method [11], results of the present study show that the dislocation density contribution in free energy change is higher.

5. Conclusions

Comparison of the XRD patterns and lattice parameter changes of the milled samples indicated that solid solution forms more effectively when the process is carried out in presence of toluene (as a PCA). Based on Miedema's model, the Gibbs free energy changes in Cu–Cr alloy systems during the formation of solid solution are calculated to be positive, which means that thermodynamic barriers exist in formation of solid solutions. However, solid solubility may be extended up to 7 wt.% Cr in Cu by 80 h of milling. In fact, the energy resulting from the milling process decreases the crystallite size and increases the crystalline defect density. Hence, the stored energy would be high enough to increase the solubility of Cr. Also, possible reasons for the difference between estimated total Gibbs free energy related to mechanical alloying and Miedema's model was discussed.

Acknowledgment

The financial support of this work by the Iran Nanotechnology Initiative Council is gratefully acknowledged.

References

- [1] Y. Jin, K. Adachi, T. Takeuchi, H.G. Suzuki, *Mater. Sci. Eng. A* 212 (1996) 149–156.
- [2] J.B. Correia, H.A. Davies, C.M. Sellars, *Acta Mater.* 45 (1997) 177–190.
- [3] M.J. Tenwick, H.A. Davies, *Mater. Sci. Eng. A* 98 (1988), 543–456.
- [4] Sh. Xi, K. Zuo, X. Li, G. Ran, J. Zhou, *Acta Mater.* 56 (2008) 6050–6060.
- [5] C. Suryanarayana, *Non-equilibrium Processing of Materials*, Pergamon Press, Oxford, 1992.
- [6] C. Suryanarayana, *Prog. Mater. Sci.* 46 (2001) 1–184.
- [7] A.N. Patel, S. Diamond, *Mater. Sci. Eng.* 98 (1988) 329–334.
- [8] D.G. Morris, M.A. Morris, *Mater. Sci. Eng. A* 104 (1988) 201–213.
- [9] K.B. Gerasimov, S.V. Mytnichenko, S.V. Pavlov, V.A. Chernov, S.G. Nikitenko, *J. Alloys Compd.* 252 (1997) 179–183.
- [10] I. Lahiri, S. Bhargava, *Powder Technol.* 189 (2009) 433.
- [11] C. Aguilar, V. de, P. Martinez, J.M. Palacios, S. Ordonez, O. Pavez, *Scr. Mater.* 57 (2007) 213–216.
- [12] G.K. Williamson, W.H. Hall, *Acta Metall.* 1 (1953) 22–31.
- [13] B.D. Cullity, S.R. Stock, *Elements of X-ray Diffraction*, third ed., Prentice Hall, Upper Saddle River, NJ, 2001.
- [14] H. Lipson, H. Steeple, *Interpretation of X-ray Powder Diffraction Patterns*, Macmillan, London, 1970.
- [15] D.R. Gaskell, *Introduction to Metallurgical Thermodynamics*, third ed., McGraw-Hill, Washington, NY, 1981.
- [16] A.R. Miedema, F.R. DeBoer, R. Boom, *Phys. B* 103 (1981) 67–81.
- [17] A.K. Niessen, A.R. Miedema, R. Andries, *Phys. Chem. Chem. Phys.* 87 (1983) 717–725.
- [18] A.K. Niessen, A.R. Miedema, F.R. de Boer, R. Boom, *Phys. B* 151 (1988) 401–432.
- [19] C. Michaelsen, C. Gente, R. Bormann, *J. Mater. Res.* 12 (1997) 1463–1467.
- [20] G.E. Dieter, *Mechanical Metallurgy*, third ed., McGraw-Hill, 1976.
- [21] F.H. Froes, C. Suryanarayana, K.C. Russell, M. Ward, *Proc. Materials Week, The Minerals, Metals & Materials Society (TMS) and the Materials Information Society*, ASM International, 1994, pp. 1–21.
- [22] Y.H. Zhao, K. Lu, K. Zhang, *Phys. Rev. B* 66 (2002) 0854041–0854048.
- [23] G.K. Williamson, R.E. Smallman, *Philos. Mag.* 1 (1956) 34–46.
- [24] R.E. Smallman, K.H. Westmacott, *Philos. Mag.* 2 (1957) 669–683.